Mitochondrial–Nuclear Communication by Prohibitin Shuttling under Oxidative Stress

ARTICLE *in* BIOCHEMISTRY · AUGUST 2011

Impact Factor: 3.02 · DOI: 10.1021/bi2008933 · Source: PubMed

7 AUTHORS, INCLUDING:

Srinivas R Sripathi
Johns Hopkins Medicine
8 PUBLICATIONS **77** CITATIONS
SEE PROFILE

Weilue He
Michigan Technological University
10 PUBLICATIONS **55** CITATIONS
SEE PROFILE

Cameron Prigge
Duke University
2 PUBLICATIONS **37** CITATIONS
SEE PROFILE

Wan Jin Jahng
American University of Nigeria
29 PUBLICATIONS **851** CITATIONS
SEE PROFILE

BIOCHEMISTRY
including biophysical chemistry & molecular biology

Article

pubs.acs.org/biochemistry

Mitochondrial–Nuclear Communication by Prohibitin Shuttling under Oxidative Stress

Srinivas R. Sripathi, Weilue He, Cameron L. Atkinson, Joseph J. Smith, Zhicong Liu, Beth M. Elledge, and Wan Jin Jahng*

Biological Sciences, Michigan Technological University, Houghton, Michigan 49931, United States

Supporting Information

ABSTRACT: Mitochondrial–nuclear communication is critical for maintaining mitochondrial activity under stress conditions. Adaptation of the mitochondrial–nuclear network to changes in the intracellular oxidation and reduction milieu is critical for the survival of retinal and retinal pigment epithelial (RPE) cells, in relation to their high oxygen demand and rapid metabolism. However, the generation and transmission of the mitochondrial signal to the nucleus remain elusive. Previously, our in vivo study revealed that prohibitin is upregulated in the retina, but downregulated in RPE cells in the aging and diabetic model. In this study, the functional role of prohibitin in the retina and RPE cells was examined using biochemical methods, including a lipid binding assay, two-dimensional gel electrophoresis, immunocytochemistry, Western blotting, and a knockdown approach. Protein depletion by siRNA characterized prohibitin as an anti-apoptotic molecule in mitochondria, while the lipid binding assay demonstrated subcellular communication between mitochondria and the nucleus under oxidative stress. The changes in the expression and localization of mitochondrial prohibitin triggered by reactive oxygen species are crucial for mitochondrial integrity. We propose that prohibitin shuttles between mitochondria and the nucleus as an anti-apoptotic molecule and a transcriptional regulator in a stress environment in the retina and RPE cells.

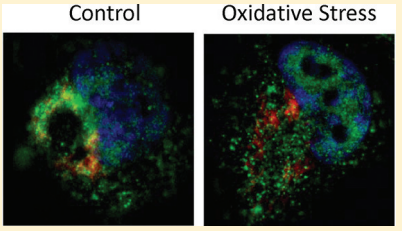

Mitochondrial–nuclear reciprocal signaling is the central question that needs to be answered to understand the maintenance mechanism of appropriate mitochondrial activities and functions in neurodegeneration. Disruptions of the mitochondrial–nuclear network lead to accelerated aging and age-related diseases. Considering the significant consequences of mitochondrial dysfunction in neurodegeneration and aging, it is crucial to understand the molecular mechanisms of mitochondrial–nuclear communication by protein shuttling.[1,2]

Cellular proteome changes, including expressions, localizations, and modifications, to adapt an oxidative environment are critical for the survival of retinal and retinal pigment epithelial (RPE) cells, because of their high oxygen demand and upregulated metabolism, especially under constant phototransduction. Oxidative stressors, including reactive oxygen species (ROS) and a hypoxic environment, are serious risk factors in retinal degeneration, including age-related macular degeneration (AMD) and diabetic retinopathy (DR). Understanding the molecular mechanisms that mediate oxidative stress-induced proteome changes and protein translocalization between mitochondria and nuclei may provide insight into pathogenesis of retinal degeneration. Previously, our proteomic study demonstrated that prohibitin is involved in oxidative stress signaling in the retina and RPE cells.[3,4] An in vivo study revealed that the aging process upregulated prohibitin in the retina and decreased its level in RPE cells. Prohibitin was first reported as an antiproliferative protein or a tumor suppressor that binds to p53, E2F, and Rb.[5,6] It forms a high-molecular mass complex with its isoform, prohibitin 2, in mitochondria.[7] Localization of prohibitin has been controversial, possibly because of cell type and extracellular stress, in being identified as mitochondrial, nuclear, or cell surface.[8,9] Prohibitin is ubiquitous in organisms ranging from bacteria to plants to humans, but its function is not clearly understood at the molecular level in each subcellular organelle.[10] Prohibitin is proposed to have roles as a cell cycle inhibitor, transcriptional regulator, inflammatory modulator, plasma membrane receptor, and mitochondrial chaperone.[6,11−18] Prohibitin plays a role in apoptosis and aging by stabilizing newly synthesized respiratory enzymes; however, its presence and function in the eye have never been elucidated.[19,20] In this study, we examined the anti-apoptotic function and the altered lipid interactions of prohibitin under oxidative stress. Translocalization of prohibitin was observed between mitochondria and the nucleus as apoptotic signaling. The changes in the expression and location of mitochondrial prohibitin triggered by redox imbalance mediated by ROS suggest a critical role of prohibitin translocalization in the maintenance of mitochondrial integrity. Here, we demonstrate that prohibitin is a new dynamic regulator of mitochondrial and nuclear functions under stress in the retina and RPE cells. Knockdown of prohibitin upregulated pro-apoptotic factors, including BAK and caspases, and decreased the levels of anti-apoptotic molecules such as BCL-xL. The significance of our study resides in our characterization

Received: June 10, 2011
Revised: August 29, 2011
Published: August 31, 2011

of prohibitin as a mitochondrion−nucleus shuttle to respond to ROS as an anti-apoptotic protein and also as a transcriptional regulator by binding to p53 in the nucleus.

MATERIALS AND METHODS

ARPE-19 Cell Culture. ARPE-19 cells were transferred to tissue culture flasks (Nunc, Roskilde, Denmark) containing Dulbecco's modified Eagle's medium (DMEM) supplemented with 10% fetal bovine serum (FBS) and 1% penicillin/streptomycin and the flasks placed in a 5% CO_2 incubator at 37 °C. After proliferation, cells were retrypsinized with a 0.1% trypsin-EDTA solution (Sigma, St. Louis, MO) for 5 min at 37 °C. After centrifugation (125*g* for 7 min), cells were plated in 24- or 6-well plates (Nunc) at a density of 2×10^4 or 8×10^4 cells/well, respectively, and allowed to grow to confluence for 2−4 days. Eight- to twelve-passage cells were used for experiments.[21,22]

Oxidative Stress Treatment. ARPE-19 cells were incubated with fresh medium for 12 h before being treated. Hydrogen peroxide (Mallinckrodt Inc.) was diluted (50, 100, 200, and 250 μM) in FBS-free medium. Cells were washed with PBS three times before being treated. Cells were treated with H_2O_2 for 1, 2, 4, 6, 8, 12, and 24 h at 37 °C in a 5% CO_2 incubator. Medium was removed immediately after the treatment, and cells were washed with PBS and harvested. Cells were lysed by RIPA buffer [0.5 M Tris-HCl (pH 7.4), 1.5 M NaCl, 2.5% deoxycholic acid, 10% NP-40, and 10 mM EDTA (Millipore)] containing protease inhibitor cocktail (Thermo Scientific) for sodium dodecyl sulfate−polyacrylamide gel electrophoresis (SDS−PAGE) and Western blot analysis or immunocytochemistry.

Immunocytochemistry. ARPE-19 cells were incubated with the final concentration of 100 nM MitoTracker Orange CMTMRos (Molecular Probes, Carlsbad, CA) in FBS-free culture medium for 30 min at 37 °C. After being washed in PBS, cells were fixed with 10% formaldehyde in PBS for 25 min at room temperature, and the membrane was permeabilized with 0.2% Triton X-100 (Sigma) in PBS for 20 min. Cells were blocked with complete medium containing 10% FBS and 0.05% Tween 20 (Sigma) for 1 h. Cells were incubated with the anti-prohibitin antibody (1:500; Genemed Synthesis Inc., San Antonio, TX) overnight at 4 °C. After being washed with PBS three times, cells were incubated with Alexa Fluor 488-conjugated anti-rabbit IgG (1:700; Molecular Probes) for 1 h at 25 °C. Finally, cells were mounted with VECTASHIELD Mounting Medium with DAPI (4,6-diamidino-2-phenylindole) to counterstain the nucleus. Images were acquired using a Zeiss AxioVert 200 M Apo Tome fluorescent microscope with 63× magnification.

Co-Immunoprecipitation. ARPE-19 cells were homogenized in lysis buffer [25 mM Tris, 120 mM NaCl, 0.3% Triton X-100, 15% glycerol, 2 mM PMSF, 10 mM EDTA, 0.2% sodium orthovanadate, and protease inhibitor cocktail]. Cells were lysed by repeated freeze−thaw cycles and sonication (3 × 5 min), followed by centrifugation at 13000*g* for 30 min. Proteins in supernatant were purified by using control agarose resin, cross-linked by 4% bead agarose, to minimize nonspecific binding. The purified anti-prohibitin antibody was immobilized with amino-linked protein A beads in the column with coupling buffer [0.5 mM sodium phosphate and 7.5 mM NaCl (pH 7.2)] and incubated with 3 μL of 5 M sodium cyanoborohydride on a shaker at 25 °C for 2 h. Columns were washed with a washing buffer [0.025 M Tris, 0.15 M NaCl, 0.001 M EDTA, 1% NP-40, and 5% glycerol (pH 7.4)]. Protein samples were incubated in the protein A−antibody column with gentle mixing overnight at 4 °C. Columns were washed three times to remove nonspecific binding proteins. Samples were equilibrated with Laemmli sample buffer containing 100 mM DTT. Eluted proteins were separated by SDS−PAGE and visualized by Western blot analysis using primary antibodies against prohibitin and p53. Protein bands on the gel were visualized by silver staining (Bio-Rad, Hercules, CA).

Two-Dimensional SDS−PAGE. Protein samples were purified with the ReadyPrep 2-D Cleanup Kit (Bio-Rad) and quantified using the BCA protein assay kit (Pierce, Rockford, IL). One hundred fifty micrograms of protein was incubated in 200 μL of rehydration buffer (8 M urea, 2 M thiourea, 2% CHAPS, and 50 mM DTT) and supplemented with 0.5% destreak IPG buffer (pH 3−10) (GE Healthcare). Isoelectric focusing was conducted using 11 cm immobiline dry strips (Bio-Rad) with linear pH 3 to 10 and pH 4 to 7 gradients. Strips were rehydrated for 12 h at 20 °C. Proteins were separated with the Ettan IPGphor-3 instrument (GE Healthcare) using programmed voltage gradients at 20 °C for a total of 12 kVh (1 h at 500 V, 1 h at 1000 V, 2 h at 6000 V, and 40 min at 6000 V). The IPG strips were reduced in equilibration buffer I [0.375 M Tris-HCl (pH 8.8), 6 M urea, 20% glycerol, 2% SDS, and 50 mM DTT] for 20 min at 25 °C and alkylated for 20 min in equilibration buffer II containing 150 mM iodoacetamide. The equilibrated strips were placed on top of polyacrylamide gels (8−16%; Bio-Rad) and sealed with 1% agarose buffer. Proteins were visualized by Coomassie staining using Imperial Protein Stain (Pierce) and Western blot analysis.

In-Gel Digestion and Mass Spectrometry. Selected protein spots from two-dimensional (2D) electrophoresis were excised from gels. The gel pieces were destained twice with 200 μL of 50% acetonitrile (MeCN)/25 mM NH_4HCO_3 buffer (pH 8.0) at room temperature for 20 min, washed once with 200 μL of 100% MeCN, and vacuum-dried with a Speed Vac concentrator (Savant, Holbrook, NY). The gel pieces were rehydrated with 13 ng/μL sequencing grade modified trypsin (Promega, Madison, WI) in 25 mM NH_4HCO_3 and incubated at 37 °C overnight. Peptides were subsequently extracted twice with 50 μL of a 50% MeCN/5% formic acid mixture for 15 min at 37 °C. All extracts were combined and dried. The peptide extracts were purified using the C18 ZipTip (Millipore). The peptides were eluted with 5 μL of a 75% MeCN/0.1% TFA mixture. The samples were analyzed by MALDI-TOF or tandem ESI MS/MS as previously described.[3,4,24−26]

Subcellular Fractionation. Bovine retinal tissues were separated and proteins isolated by the Cox and Emili method, which uses different centrifugation in density gradients to generate nuclear, mitochondrial, and cytosolic protein components.[27] Cold PBS-prerinsed tissue was homogenized in homogenization buffer and centrifuged at 800*g* for 15 min. The pellet was resuspended for further isolation of nuclear proteins. The supernatant was collected and centrifuged at 6000*g* for 15 min. The pellet was saved for mitochondria and supernatant for cytosol−microsome separation. The crude nuclear fraction was suspended in nuclear extraction buffer and separated by ultracentrifugation at 80000*g* for 35 min. To obtain mitochondrial membrane and matrix protein, the pellet was resuspended in membrane extraction hypotonic lysis buffer centrifuged at 9000*g* for 30 min. Cytosolic proteins were obtained by spinning the supernatant for 1 h at 100000*g*.

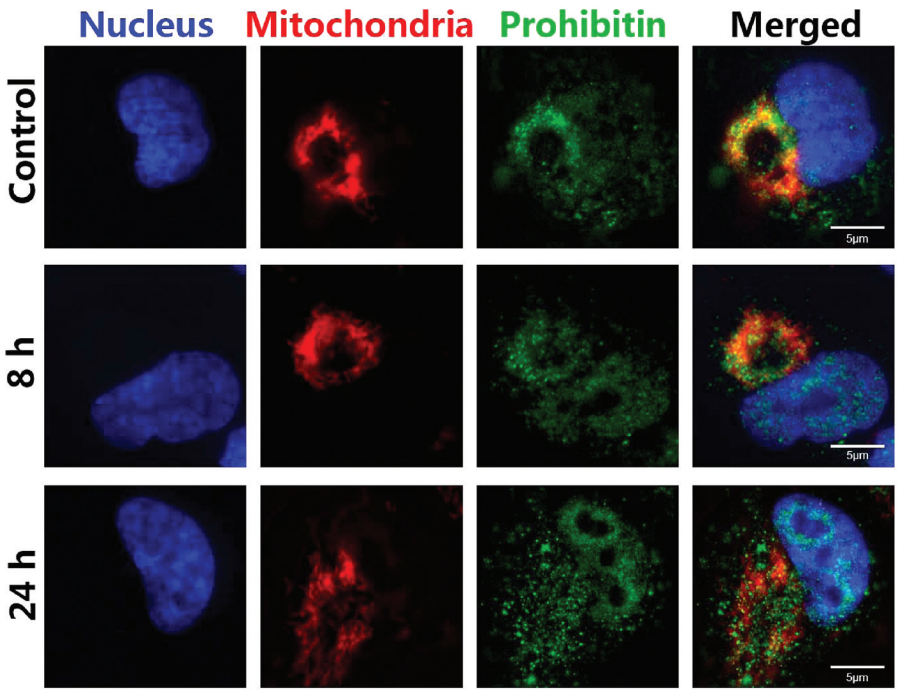

Figure 1. Translocalization of prohibitin under oxidative stress. ARPE-19 cells treated with H_2O_2 (200 μM for 8 or 24 h) were analyzed by immunocytochemistry. Subcellular organelles and prohibitin were visualized by DAPI (blue, nucleus), the prohibitin-specific primary antibody, the Alexa Fluor 488-conjugated secondary antibody (green, prohibitin), and MitoTracker Orange (red, mitochondria). Prohibitin was translocalized from mitochondria to the nucleus under oxidative stress in a time-dependent manner. The scale bar is 5 μm.

SDS–PAGE and Western Blot Analysis. Protein quantification was conducted with the BCA protein assay kit (Pierce). Samples were dissolved in Laemmli sample buffer [62.5 mM Tris-HCl (pH 6.8), 25% glycerol, 2% SDS, and 0.01% bromophenol blue]. Proteins were resolved using 8 to 16% polyacrylamide precast gels (Bio-Rad), followed by electrotransfer onto the methanol-activated PVDF membrane, and blocked in 5% nonfat milk prepared in TTBS [0.1% (v/v) Tween 20] for 1 h at 25 °C. The membranes were incubated with primary antibodies at 4 °C overnight and subsequently incubated with corresponding horseradish peroxidase-conjugated secondary antibodies for 1 h at 25 °C. Proteins were visualized by using West Pico Chemiluminescent Substrate (Pierce). Immunoreactive protein bands were acquired using a LAS 4000 mini luminescent image analyzer and quantified using Quantity One (Bio-Rad). Proteins in gels were stained with Imperial Protein Stain and scanned using a GS800 imaging densitometer (Bio-Rad).

Lipid–Protein Interaction Assay. Lipid strips were purchased from Echelon Biosciences or prepared using a nitrocellulose membrane in the lab. For commercially available lipid strips, membranes with a solvent blank control and 15 different lipids were initially blocked with SuperBlock (Pierce) blocking buffer for 1 h at room temperature. To prepare our own lipid strips, we spotted different amounts of lipids (100 pmol to 10 nmol), including cardiolipin, cholesterol, and phosphatidylserine, onto the nitrocellulose membrane. The membrane was air-dried for 1 h at room temperature. Crude proteins, fractionated samples, or prohibitin partially purified by co-IP (1 μg/mL) from control ARPE-19 cells or cells under oxidative stress (200 μM H_2O_2) was incubated with a nitrocellulose membrane overnight. The membrane was washed three times with TTBS buffer [Tris-buffered saline with 0.1% (v/v) Tween 20], followed by incubation with the prohibitin antibody (1:1000; Genemed Synthesis Inc.) overnight at 4 °C with gentle agitation. Blots were washed with TTBS buffer and incubated with horseradish peroxidase-conjugated anti-rabbit secondary antibody (1:10000; Agrisera, Vännäs, Sweden) for 1 h at 25 °C. Strips were developed with Super Signal West Pico Chemiluminescence Substrate (Pierce), and proteins were visualized using a LAS 4000 mini luminescent image analyzer (Fuji).

siRNA Transfection. ARPE-19 cells were seeded in 24-well plates at a density of 6×10^4 cells/well with 0.1 mL of DMEM containing 10% FBS and 1% penicillin/streptomycin. Cells were incubated at 37 °C with 5% CO_2. Cells were treated with 175 ng (final concentration of 23 nM) of siRNA (AAAGCCAGCTTCCTCGCATCT) against prohibitin (Flexi-iTube siRNA) and random sequence control siRNA in 100 μL of culture medium without serum. Transfection was conducted with HiPerFect transfection reagent (Qiagen, Valencia, CA), and cells were harvested 48 h post-transfection. Proteins were assayed by Western blot for detection of AIF (EMD Millipore), BCL-xL (sc-634; Santa Cruz Biotechnology), caspase-9 (AB16969; EMD Millipore), BAK (ab32371; Abcam), and actin (sc-47778; Santa Cruz Biotechnology). Protein localizations and expressions were also analyzed by immunocytochemistry.

RESULTS

Mitochondrial–Nuclear Trafficking of Prohibitin. Oxidative stress induced by hydrogen peroxide has been implicated in many ocular diseases. RPE cells maintain a reducing environment within cells to balance the production of reactive oxygen species and detoxification. Recently, we studied early molecular signaling events during oxidative stress in the retina and RPE cells using a comparative proteomics approach to identify altered protein levels.[3,4,23–26] In RPE cells, one of

dx.doi.org/10.1021/bi2008933 | Biochemistry 2011, 50, 8342–8351

the downregulated proteins under oxidative stress was prohibitin. Changes in the prohibitin level in both diabetic and aging eyes suggest that it may have an apoptosis-related function in RPE cells, especially under chronic stress and pathophysiological conditions.[3]

First, we examined the cellular localization of prohibitin, which is a controversial question. Translocalization of prohibitin in response to oxidative stress was examined using immunocytochemistry. Subcellular organelles and prohibitin were visualized by DAPI (nuclear DNA, blue, 369 and 460 nm for absorbance and emission, respectively), MitoTracker Orange (mitochondria, red, 578 and 599 nm for absorbance and emission, respectively), and Alexa Fluor 488 (prohibitin, green, 495 and 519 nm for absorbance and emission, respectively), by taking three color fluorescent images every hour. A kinetic assay confirmed that the signaling pathway was involved in the movement of prohibitin to the nucleus from mitochondria. Confluent ARPE-19 cells were treated with 200 μM H_2O_2 for 24 h. H_2O_2-treated cells showed nuclear translocalization of prohibitin, whereas untreated cells showed localization in mitochondria (Figure 1). After 8 h, prohibitin showed an accumulation in the nucleus as compared to the control group. After 24 h, more nuclear prohibitin was observed and much less colocalized with mitochondria.

To examine prohibitin response in apoptosis signaling in detail, we then examined changes in the protein expression level in vitro using ARPE-19 cells. We examined changes in the prohibitin level under H_2O_2 in a time- and dose-dependent manner. Protein analysis by SDS−PAGE and Western blotting demonstrated that prohibitin is downregulated under oxidative stress (200 μM H_2O_2 for 1−24 h) (Figure 2). Cells treated with

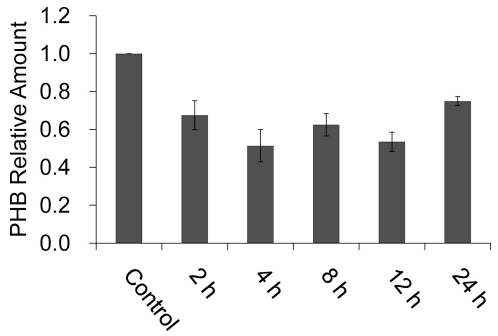

Figure 2. Downregulation of prohibitin under oxidative stress. ARPE-19 cells were treated with H_2O_2. At specific time points, cells were harvested and proteins separated by SDS−PAGE. Prohibitin was visualized by Western blotting. The level of prohibitin decreased in all treated groups. ANOVA was used to demonstrate the differences among groups. Statistical analysis showed that there is a significant difference among groups ($P < 0.01$). Tukey's Honestly Significant Difference (HSD) test was applied to find the source of the difference. Results showed that control group was significantly different from the treated groups (4 and 12 h, $P < 0.01$; 2, 8, and 24 h, $P < 0.05$). No significant difference was found among treated groups.

200 μM H_2O_2 showed a 40% decrease in their level of prohibitin, but the levels between treated groups after 24 h revealed no significant difference by t test, indicating that a decreased level of prohibitin caused by oxidative stress is an acute process that occurs within 2 h. Downregulation of prohibitin under stress conditions suggests that the nuclear prohibitin may not be a newly synthesized protein as there was no increase in the level of prohibitin for 24 h; the nuclear prohibitin might derive from mitochondria because prohibitin was not colocalized with mitochondria after extended H_2O_2 treatment.

To address the issue of the membrane binding property of prohibitin in RPE cells, we investigated the effect of stress on protein solubility. First, we examined the correlation between oxidative stress and soluble prohibitin and found that the ratio of soluble prohibitin to membrane binding prohibitin decreased under oxidative stress. Prohibitin exists in both detergent-resistant insoluble and soluble fractions and was separated by SDS−PAGE using 8 to 16% gradient gels and the maximal running time. Membrane-binding prohibitin showed slightly higher molecular mass when compared to that of soluble prohibitin. As shown in panels A and B of Figure 3, the level of

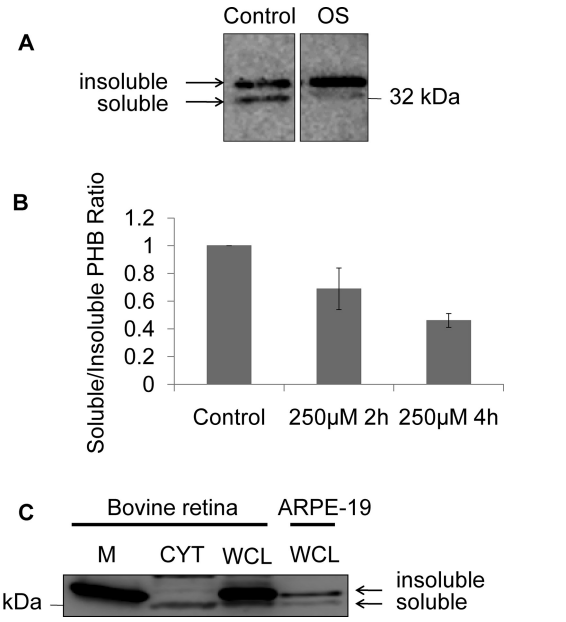

Figure 3. Detergent-resistant membrane prohibitin under oxidative stress. (A) Detergent-resistant (insoluble) and soluble prohibitins were separated by SDS−PAGE and visualized by Western blotting. Under oxidative stress (OS, 250 μM H_2O_2, 4 h), detergent-resistant prohibitin was upregulated compared to the control. (B) Quantitative analysis of insoluble and soluble prohibitin under oxidative stress. (C) Prohibitins from bovine retinal cells and ARPE-19 cells were compared for the analysis of insoluble and soluble forms. Mitochondrial prohibitin (M) moved slightly slower than the cytosolic form (CYT). Whole cell lysate (WCL) from both bovine retinal cells and ARPE-19 cells shows detergent-resistant insoluble and soluble forms of prohibitin.

soluble prohibitin from ARPE-19 cells decreased and the level of detergent-resistant, membrane-binding insoluble prohibitin increased under stress conditions in 4 h. To compare insoluble and soluble forms from subcellular organelles, we separated prohibitins from mitochondria (M), cytosol (CYT), and whole cell lysate (WCL) by SDS−PAGE and visualized them by Western blotting (Figure 3C). Soluble prohibitin from ARPE-19 cells in the cytosolic fraction (32 kDa) moved faster than membrane-bound mitochondrial and microsomal prohibitin (34 kDa). The insoluble, detergent-resistant, membrane-binding prohibitin exhibited a slightly higher-molecular mass band compared to that of cytosolic, soluble prohibitin. Prohibitins in whole cell lysate from both retinal and RPE cells showed two bands as insoluble and soluble forms. It is possible that the membrane-binding and soluble prohibitins

dx.doi.org/10.1021/bi2008933 | Biochemistry 2011, 50, 8342−8351

may exist in different subcellular organelles, so we next examined the subcellular localization of prohibitin.

Subcellular Localization of Prohibitin in the Retina and RPE Cells. Our previous experiments demonstrated that prohibitin may respond differently in the retina and RPE cells under various oxidative stress conditions, including diabetes and aging. To specify the location of prohibitin in the retina, we fractionated bovine retina using serial centrifugation and specific detergents, including polyamines.[27] Via this method, proteins were separated by nuclear and mitochondrial extraction buffer. Denatured and native gel electrophoresis and Western blotting of the subcellular organelle showed that prohibitin is widely distributed in retina cells but centralized in mitochondria (Figure 4). We used cytochome *c*, RNA

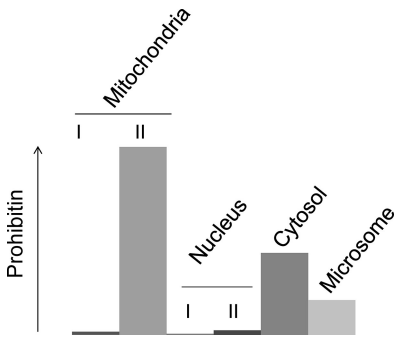

Figure 4. Subcellular localization of prohibitin. Subcellular fractions were separated by the Cox and Emili method. Proteins in the retina were fractionated on the basis of serial centrifugations with extraction buffers and separated by SDS–PAGE. The prohibitin concentration was quantitatively analyzed. Prohibitin in bovine retina was localized mostly in mitochondria as a membrane-associated form (II, mitochondrial membrane) rather than a soluble form (I, mitochondrial matrix). Prohibitin was also detected in the nucleus. The relative amounts of prohibitin are presented as matrix (I) and membrane (II) in mitochondria, nucleus (supernatant I and membrane-associated II), cytosol, and microsome.

polymerase II, and transketolase as positive controls to show mitochondrial, nuclear, and cytosolic fractions, respectively (Figure 1 of the Supporting Information). Quantitative analysis showed that 60–80% of prohibitin in bovine retina was localized in the mitochondrial membrane pellet (Figure 4, Mitochondria II) in bovine retina cells, but the cytosol and nucleus (soluble I and membrane II) also contain a substantial amount of prohibitin. Then we explored the prohibitin levels in different subcellular locations in RPE cells. Our fractionation experiments using ARPE-19 cells showed that prohibitin has a membrane-binding and soluble form. In ARPE-19 cells, prohibitin was mainly expressed in mitochondria (60–80%) as determined by the Cox fractionation method.[27]

As prohibitin is widely spread in each subcellular fraction, we asked whether different subcellular prohibitins have the same isoelectric point (pI). We used 2D electrophoresis to isolate prohibitin from the fractionated subcellular proteome. Mitochondrial, nuclear, cytosolic, and microsomal prohibitin were separated and visualized by Coomassie staining and Western blotting (Figure 5). In the mitochondrial fraction, prohibitin exhibited a molecular mass of 32 kDa and a pI of 5.6 as expected. Prohibitin was more acidic in the nucleus, with a pI of 5.3, because of post-translational modifications such as phosphorylation. Cytosolic prohibitin showed very basic spots

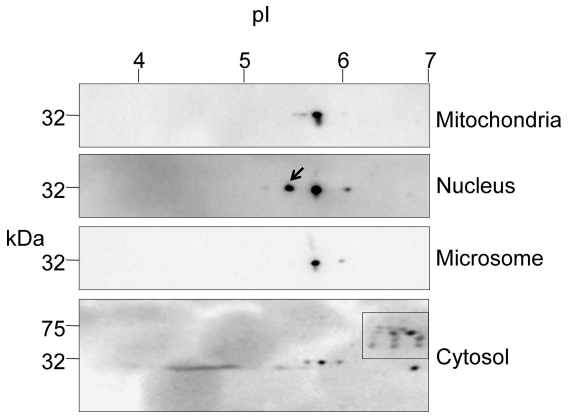

Figure 5. 2D SDS–PAGE analysis of prohibitin. Each fraction from bovine retinal cells was separated by isoelectric focusing and gel electrophoresis. Prohibitin was visualized by Western blotting. The nuclear fraction showed phosphorylated prohibitin as one acidic spot at pI 5.3 shown by the arrow, whereas many modified prohibitin spots in the box were detected in the cytosolic fraction.

of pI 6–7 and a higher molecular mass as shown in the box, representing potential ubiquitination.

As each subcellular prohibitin exhibited different pI values in 2D electrophoresis, we examined potential post-translational modifications in bovine retinal cells, including phosphorylation, using a different fractionation method.[27] Mitochondrial and nuclear fractions were further separated by matrix or supernatant (Mito I and Nucl I) versus membrane (Mito II and Nucl II) proteins. Prohibitin in the mitochondrial matrix (Figure 6A, lane 1) and cytosol (Figure 6A, lane 5) may exist as a putative heterodimer at 75 kDa, whereas it showed multiple bands around 32 kDa in the nucleus and cytosol, possibly because of phosphorylation or peripheral membrane interactions. Proteins in each fraction were separated by electrophoresis, and prohibitin was visualized by Western blotting using prohibitin and phosphatidylserine (p-Ser) antibodies. Only the nuclear fraction exhibited phosphorylated prohibitin demonstrated by p-Ser Western blot (Figure 6A, lanes 9 and 10). Mitochondrial, cytosolic, and microsomal prohibitins did not show phosphorylation. To confirm these data, we performed native gel electrophoresis and produced the same result (Figure 6B, lanes 9 and 10). Mass spectrometry (MALDI-TOF-TOF) analysis revealed that S101 and S151 sites are phosphorylated (data not shown).

Prohibitin Binds Cardiolipin under Oxidative Stress. We next asked whether prohibitin localization could be controlled by membrane lipid binding. Considering mitochondrion-specific lipid composition, we speculated that the localization and trafficking of prohibitin might be determined by a mitochondrion-specific lipid such as cardiolipin. Prohibitin in the bovine retina binds with cardiolipin, a major mitochondrial phospholipid (Figure 7A). The lipid interaction assay demonstrated that mitochondrial prohibitin from bovine retina has a strong affinity at relatively low cardiolipin concentrations (10–15 μg, 6–10 nmol), whereas nuclear prohibitin showed a weaker affinity for cardiolipin (Figure 7B).

However, prohibitins in RPE cells showed different lipid interactions under oxidative stress when we examined prohibitin using ARPE-19 cells. Under normal conditions, prohibitin from ARPE-19 cells demonstrated a strong interaction with phosphatidylinositol 3,4,5-triphosphate (PIP3) but not with cardiolipin (Figure 8). The lipid binding

dx.doi.org/10.1021/bi2008933 | *Biochemistry* 2011, 50, 8342–8351

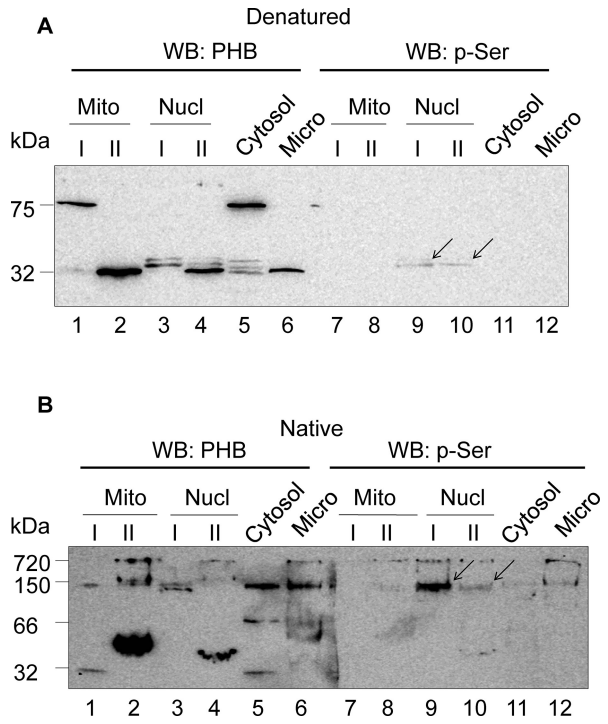

Figure 6. Phosphorylation of prohibitin in the nucleus. (A) Each fraction was further separated by SDS–PAGE and phospho-Western blotting. Prohibitin in the mitochondrial matrix (I) and cytosol shows a putative heterodimer at 75 kDa under denaturing conditions, whereas nuclear prohibitin (supernatant I and membrane II) shows multiple bands due to modifications and membrane association. Prohibitin in the nuclear fraction was phosphorylated as shown by using the p-Ser antibody (lanes 9 and 10). (B) Proteins were separated by native gel electrophoresis, and prohibitin was visualized by Western blotting using the anti-prohibitin primary antibody and p-Ser antibody. Prohibitin in the nucleus is phosphorylated as shown in lanes 9 and 10. Prohibitin may exist as a heterodimer or oligomer as shown in lane 2 (mitochondrial membrane, 50, 150, and 750 kDa), lane 3 (nuclear supernatant, 150 kDa), lane 5 (cytosol, 75 and 150 kDa), and lane 6 (microsome, 150 kDa).

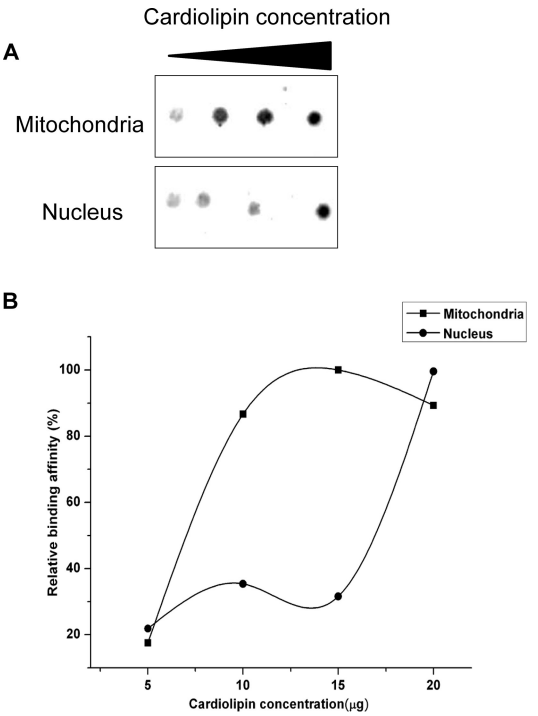

Figure 7. Prohibitin–cardiolipin interactions. (A) Prohibitin in the nucleus and mitochondria from bovine retina showed different cardiolipin affinities depending on the cardiolipin concentration. (B) Quantitative analysis of prohibitin–cardiolipin binding. Data for mitochondrial prohibitin (■) and nuclear prohibitin (●) are shown. The *Y*-axis represents the relative binding affinity and the *X*-axis the cardiolipin concentration.

affinity changed dramatically under oxidative stress induced by H_2O_2 (200 μM). Prohibitin under stress showed a strong affinity for cardiolipin as shown in Figure 8. This observation led us to conclude that prohibitin has an affinity for negatively charged phospholipids, especially cardiolipin. Lipid analysis by mass spectrometry demonstrated that the cardiolipin concentration decreased 20–70% under 200 μM H_2O_2 (data not shown).

Anti-Apoptotic Prohibitin Function in Mitochondria. We performed a loss of function study with prohibitin-specific small interfering RNA (siRNA), resulting in an increase in the level of apoptotic signaling at decreased prohibitin levels (Figure 9). We tested two siRNA constructs that inhibit prohibitin expression against a control siRNA that has a random sequence. A solvent vehicle was used as a negative control. We chose conditions under which the levels of prohibitin expression were reduced by 80–90% when compared to the random sequence control. We examined whether anti-apoptotic molecules such as BCL-xL and pro-apoptotic molecules that include apoptosis inducing factor (AIF), caspases, and BCL-2 homologous antagonist/killer (BAK) are also activated as essential markers in apoptosis (Figure 9A). The activation of AIF and caspase-9 cleavage, the upstream regulators in apoptosis, showed early apoptotic signaling under prohibitin knockdown conditions. However, the level of anti-apoptotic BCL-xL decreased when prohibitin was downregulated. Further, we investigated whether prohibitin knockdown cleaves poly(ADP ribose) polymerase (PARP) as a pro-apoptotic marker. PARP cleavage is an early marker of caspase activation. Transfection of siRNA of prohibitin into ARPE-19 cells resulted in an increased level of cleavage of PARP, which represents the fact that an apoptotic signal is induced when prohibitin is downregulated (data not shown). Our results demonstrate that knockdown of prohibitin increases the strength of apoptotic signaling. These observations suggest that prohibitin may act as an anti-apoptotic protein in mitochondria by forming a functional complex with apoptotic proteins. The prohibitin concentration is inversely correlated with the initiation of apoptosis. Then we examined whether a decreased level of prohibitin disrupts the filamentous reticular network of mitochondria and results in fragmented mitochondria. Immunocytochemical analysis showed that prohibitin knockdown led to accumulation of fragmented mitochondria as shown in Figure 9B. Fragmented mitochondria imply that the fusion of mitochondrial membranes is impaired when the prohibitin concentration is decreased.

Prohibitin Function in the Nucleus. To address a putative functional role of prohibitin in the nucleus, protein–protein interaction was examined. Immunoprecipitation of prohibitin demonstrated that prohibitin is involved in direct regulation of transcription through p53 binding. The prohibitin–protein binding assay using the anti-prohibitin primary antibody, followed by SDS–PAGE, and mass spectrometry demonstrated that prohibitin has interactions

dx.doi.org/10.1021/bi2008933 | *Biochemistry* 2011, 50, 8342–8351

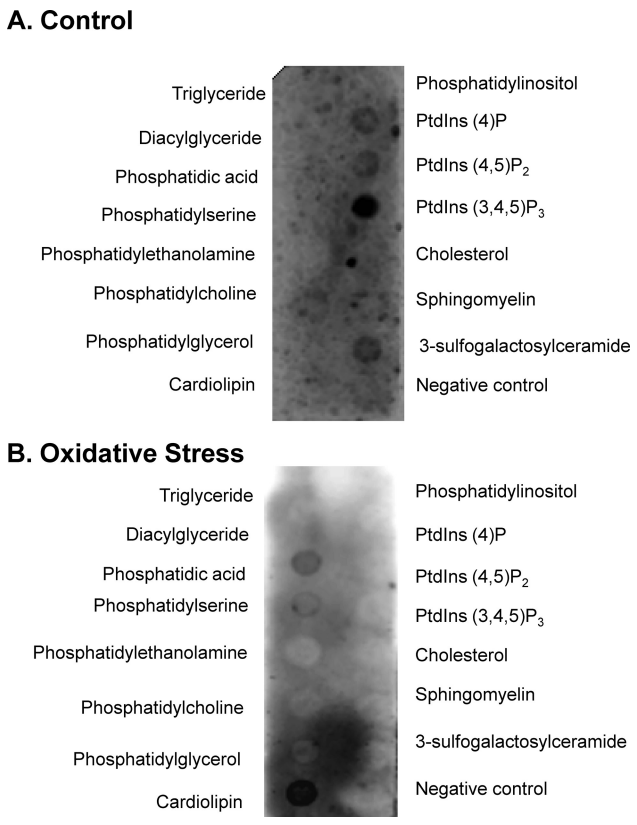

Figure 8. Fractionated or IP-purified proteins were incubated with the nitrocellulose membrane coated with various lipids. The membrane was incubated with immunoprecipitated prohibitin, and the lipid–prohibitin interaction was visualized by Western blotting. Prohibitin–lipid binding was changed under oxidative stress (200 μM H_2O_2). Under normal conditions, prohibitin interacts with phosphatidylinositol phosphates (PIP3), whereas under oxidative stress, prohibitin binds with cardiolipin.

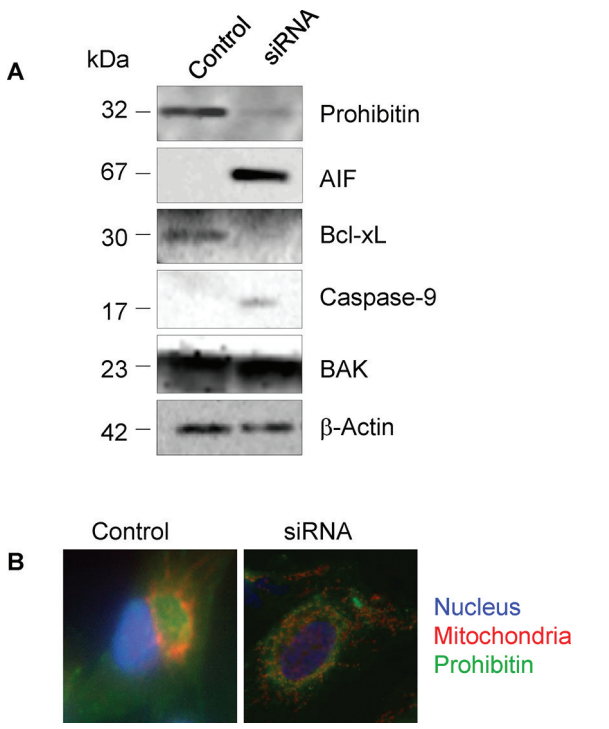

Figure 9. Anti-apoptotic prohibitin shown by knockdown analysis. (A) ARPE-19 cells were transfected by siRNA and random sequence. The level of anti-apoptotic BCL-xL increased when prohibitin was downregulated. Pro-apoptotic proteins, including AIF, caspase-9, and BAK, were upregulated under prohibitin knockdown conditions. (B) ARPE-19 cells under siRNA or random sequence were analyzed by immunocytochemistry. Prohibitin, mitochondria, and the nucleus were visualized by Alexa Fluor 488 (green), MitoTracker Orange (red), and DAPI (blue), respectively. When prohibitin was downregulated by siRNA, the mitochondrial structure was disrupted, and mitochondrial prohibitin was moved to the nuclear membrane.

with transcription factors that include tumor suppressor p53. A Western blot of immunoprecipitated fractions confirmed prohibitin–p53 interaction as shown in Figure 10. To test oxidized cardiolipin-dependent translocalization, we examined a known cardiolipin antioxidant etoposide. Etoposide is an antitumor drug that acts as a topoisomerase II inhibitor and is used to block cardiolipin oxidation and prohibitin translocalization. Treatment for 1 h induced translocalization of prohibitin from the nucleus to the cytosol (Figure 2 of the Supporting Information).

DISCUSSION

In this study, we demonstrate that prohibitin is translocalized from mitochondria to the nucleus as a mitochondrial response to oxidative stress in vitro. Previously, we investigated oxidative stress-induced proteome changes in RPE cells using the differential gel electrophoresis (DIGE) technique to identify early biomarkers of eye diseases.[3,4] We were seeking a novel protein that shuttles between mitochondria and the nucleus as the initiation step in retinal pathogenesis. We found that prohibitin changes its subcellular location under stress conditions. In this study, dynamic translocalization of prohibitin was examined by subcellular fractionation, immunocytochemistry, a lipid binding assay, and a knockdown approach. This study challenges a question of mitochondrial–nuclear (MT–NU) communication by protein translocalization through the

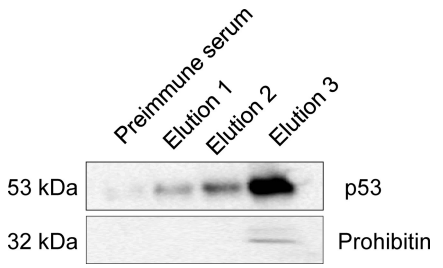

Figure 10. Binding of prohibitin to p53. Immunoprecipitation using the prohibitin antibody demonstrated the interaction between prohibitin and p53. The purified anti-prohibitin antibody was immobilized with amino-linked protein A and washed. Protein samples were incubated in the protein A–antibody column with gentle mixing overnight at 4 °C. Columns were washed three times to remove nonspecific binding proteins. Eluted fractions were separated by SDS–PAGE and visualized by Western blotting using primary antibodies against prohibitin and p53.

lipid interaction change mechanism. Knockdown and immunoprecipitation studies suggest that trafficking prohibitin may have a dual function as an anti-apoptotic molecule that maintains mitochondrial structure and as a transcriptional activator that interacts with p53 in the nucleus. We tested the hypothesis that a lipid binding property of prohibitin may determine mitochondrial localization. As prohibitins are expected to be dynamically translocated within retinal and

dx.doi.org/10.1021/bi2008933 | Biochemistry 2011, 50, 8342–8351

RPE cells, there is an essential need for a time-dependent assay of cellular prohibitin movement. Under oxidative stress, the level of cardiolipin decreased and the level of cardiolipin–prohibitin interactions increased. At relatively low cardiolipin concentrations (<6–10 nmol), mitochondrial prohibitin competes with nuclear prohibitin for cardiolipin binding. We examined whether levels of prohibitin in mitochondria and the nucleus are altered by oxidative stress. We found that the level of prohibitin initially decreased by mild oxidative stress with H_2O_2 treatment especially at the IC_{50} concentration.[3,23] Translocalization of prohibitin under stress conditions led us to investigate post-transcriptional regulation. A proteomics approach using SDS–PAGE and phospho-Western blotting demonstrated that soluble nuclear prohibitin is phosphorylated. Gel electrophoresis under denatured or native conditions showed that prohibitin may exist as a heterodimer, soluble, membrane-associated, and post-translationally modified form in different subcellular organelles. Upregulation of pro-apoptotic molecules and downregulation of anti-apoptotic proteins under prohibitin depletion by siRNA suggest an anti-apoptotic response of prohibitin depending on the prohibitin levels.

To maintain mitochondrial integrity, nuclear and mitochondrial genes should communicate with each other, especially under stress conditions that include hypoxia, abnormal temperature, nutrient deficiency, and aging. Our results suggest that prohibitin may fulfill dual roles as a phospholipid scaffold switch and an MT–NU shuttle under stress conditions in the retina and RPE cells. Coordinated prohibitin–lipid interactions, including cardiolipin and PIP3, support the phospholipid scaffold switch mechanism hypothesis.[28,29] Cardiolipin, a negatively charged diphosphatidylglycerol-derived phospholipid, is mainly localized in mitochondria and plays a significant role in maintaining mitochondrial membrane function and structure. The level of cardiolipin decreases with aging and is involved in the upregulation of mitochondrially derived reactive oxygen species. Considering cardiolipin's role in mitochondria, it is reasonable to speculate that cardiolipin composition may affect targeted trafficking of mitochondrial proteins, especially under oxidative stress. The age-related decrease in the level of cardiolipin is correlated with an increased cholesterol:phospholipid ratio.[30] Cholesterol depletion using β-cyclodextrin and simvastatin upregulated prohibitin expression, and cholesterol treatment decreased the level of prohibitin in ARPE-19 cells (data not shown). Post-translational modifications that include hydrophobic palmitoylation and negatively charged phosphorylation may affect membrane binding and translocalization in subcellular organelles.[25,31–33]

Consistent with our results, recent studies using pro-apoptotic peptide targeting prohibitin demonstrated that prohibitin might be connected to upregulation of lipid turnover and an increased metabolic rate.[14] Changes in cellular metabolism are a central hallmark in the aging process in the retina and RPE cells. When apoptosis was induced by prohibitin–peptide binding, it was shown that the levels of lipid metabolism, energy expenditure, oxygen consumption, and heat generation increased. Using *Caenorhabditis elegans* as a model system, it was reported that prohibitin depletion affected ATP levels, lipid content, and mitochondrial proliferation in an age-specific manner.[34] Our results support the hypothesis that prohibitin may have a similar role in modulating mitochondrial structure by binding cardiolipin to maintain mitochondrial integrity under stress conditions. This study also demonstrated that prohibitin expression levels may determine the mitochondrial morphology and distribution as shown by the knockdown approach.

Recent studies examined the versatile functions of prohibitin as a drug resistance mediator, plasma membrane receptor, obesity regulator, and cancer target.[14,35–40] A metabolic switch mechanism of prohibitin was shown by pyruvate carboxylase inhibition and PIP3 binding.[41] Prohibitin may modulate glucose and fatty acid oxidation by balancing between oxidative phosphorylation and anaerobic glycolysis under rapid proliferation, which are associated with malignant transformation.[42] Downregulation of prohibitin may activate a retrograde communication that induces mitochondrial proliferation and an increased level of reactive oxygen species (ROS).[30,34,43–48]

A functional role for prohibitin in the nucleus was suggested as a transcriptional regulator by observation of its interactions with p53, E2F, and Rb.[47] In cancer cells, prohibitin is localized in the nuclear matrix.[49] Cholesterol-induced downregulation of prohibitin was shown as a regulator of cell cycle transit in the nucleus.[45,50] Our previous study suggested that NF-κB was translocated into the nucleus under oxidative stress, and protein translocalization may act as a cell survival mechanism under stress conditions.[3] Nuclear tumor suppressor p53 also translocalized into mitochondria under apoptotic conditions. The coordinated translocalization of prohibitin may determine cell viability and the apoptotic cell population in the retina and RPE cells. Prohibitin under oxidative stress and altered lipid environments may regulate the cell survival or death pathway by changing protein–lipid interactions. In the beginning of retinal degeneration, prohibitin may act as an anti-apoptotic molecule as the default function in mitochondria, whereas it may become a transcriptional regulator under prolonged or repeated stress conditions. This dual function of prohibitin might be the essential mechanism for controlling apoptotic signaling as a cell fate determinant from uncontrolled proliferation as suggested by the conserved gene evolution in an oxidative environment.[51]

■ ASSOCIATED CONTENT

Ⓢ Supporting Information

In Figure 1, to confirm the efficiency of subcellular fractionation, positive markers in subcellular organelles were analyzed by Western blotting. Proteins were fractionated by the Cox and Emili method and separated by SDS–PAGE. RNA polymerase II, transketolase, and cytochrome *c* were used as the nuclear (N), cytosolic (C), and mitochondrial (M) markers, respectively. Figure 2 shows translocalization of prohibitin under oxidative stress and mitochondrial protection by etoposide treatment. This material is available free of charge via the Internet at http://pubs.acs.org.

■ AUTHOR INFORMATION

Corresponding Author

*Phone: (906) 487-2192. Fax: (906) 487-3167. E-mail: wjahng@mtu.edu.

Author Contributions

S.R.S. and W.H. contributed equally to this work.

Funding

This study was supported by the Century II Equipment fund and the Research Excellence Fund of Michigan Technological University.

■ ACKNOWLEDGMENTS

We thank Drs. Ramakrishna Wusirika, Mi Hye Song, Jeremy Goldman, Mike Gibson, and Manuela Bartoli for insightful discussions and sharing equipment. We thank Jackie Pribyl, Aram Kim, and Sulagna Gupta for their excellent technical assistance. Matthew Durocher is acknowledged for his suggestions and critical reading.

■ ABBREVIATIONS

AMD, age-related macular degeneration; DAPI, 4′,6-diamidino-2-phenylindole; DIGE, differential gel electrophoresis; DMEM, Dulbecco's modified Eagle's medium; DR, diabetic retinopathy; IP, immunoprecipitation; PARP, poly(ADP ribose) polymerase; ROS, reactive oxygen species; RPE, retinal pigment epithelial; siRNA, small interfering RNA.

■ REFERENCES

(1) Ryan, M. T., and Hoogenraad, N. J. (2007) Mitochondrial-nuclear communications. *Annu. Rev. Biochem. 76*, 701−722.

(2) Cannino, G., Di Liegro, C. M., and Rinaldi, A. M. (2007) Nuclear-mitochondrial interaction. *Mitochondrion 7*, 359−366.

(3) Lee, H., Arnouk, H., Sripathi, S., Chen, P., Zhang, R., Bartoli, M., Hunt, R. C., Hrushesky, W. J., Chung, H., Lee, S. H., and Jahng, W. J. (2010) Prohibitin as an oxidative stress biomarker in the eye. *Int. J. Biol. Macromol. 47*, 685−690.

(4) Arnouk, H., Lee, H., Zhang, R., Chung, H., Hunt, R. C., and Jahng, W. J. (2011) Early biosignature of oxidative stress in the retinal pigment epithelium. *J. Proteomics 74*, 254−261.

(5) McClung, J. K., Danner, D. B., Stewart, D. A., Smith, J. R., Schneider, E. L., Lumpkin, C. K., Dell'Orco, R. T., and Nuell, M. J. (1989) Isolation of a cDNA that hybrid selects antiproliferative mRNA from rat liver. *Biochem. Biophys. Res. Commun. 164*, 1316−1322.

(6) Nijtmans, L. G., de Jong, L., Artal Sanz, M., Coates, P. J., Berden, J. A., Back, J. W., Muijsers, A. O., van der Spek, H., and Grivell, L. A. (2000) Prohibitins act as a membrane-bound chaperone for the stabilization of mitochondrial proteins. *EMBO J. 19*, 2444−2451.

(7) Steglich, G., Neupert, W., and Langer, T. (1999) Prohibitins regulate membrane protein degradation by the m-AAA protease in mitochondria. *Mol. Cell. Biol. 19*, 3435−3442.

(8) Wang, S., Fusaro, G., Padmanabhan, J., and Chellappan, S. P. (2002) Prohibitin co-localizes with Rb in the nucleus and recruits N-CoR and HDAC1 for transcriptional repression. *Oncogene 21*, 8388−8396.

(9) Rivera-Milla, E., Stuermer, C. A., and Málaga-Trillo, E. (2006) Ancient origin of reggie (flotillin), reggie-like, and other lipid-raft proteins: Convergent evolution of the SPFH domain. *Cell. Mol. Life Sci. 63*, 343−357.

(10) McClung, J.K., Jupe, E. R., Liu, X. T., and Dell'Orco, R. T. (1995) Prohibitin: Potential role in senescence, development, and tumor suppression. *Exp. Gerontol. 30*, 99−124.

(11) Wang, S., Nath, N., Fusaro, G., and Chellappan, S. (1999) Rb and prohibitin target distinct regions of E2F1 for repression and respond to different upstream signals. *Mol. Cell. Biol. 19*, 7447−7460.

(12) Wang, S., Nath, N., Adlam, M., and Chellappan, S. (1999) Prohibitin, a potential tumor suppressor, interacts with RB and regulates E2F function. *Oncogene 18*, 3501−3510.

(13) Sharma, A., and Qadri, A. (2004) Vi polysaccharide of *Salmonella typhi* targets the prohibitin family of molecules in intestinal epithelial cells and suppresses early inflammatory responses. *Proc. Natl. Acad. Sci. U.S.A. 101*, 17492−17497.

(14) Kolonin, M. G., Saha, P. K., Chan, L., Pasqualini, R, and Arap, W. (2004) Reversal of obesity by targeted ablation of adipose tissue. *Nat. Med. 10*, 625−632.

(15) Patel, N., Chatterjee, S. K., Vrbanac, V., Chung, I., Mu, C. J., Olsen, R. R., Waghorne, C., and Zetter, B. R. (2010) Rescue of paclitaxel sensitivity by repression of Prohibitin1 in drug-resistant cancer cells. *Proc. Natl. Acad. Sci. U.S.A. 107*, 2503−2508.

(16) Artal-Sanz, M., Tsang, W. Y., Willems, E. M., Grivell, L. A., Lemire, B. D., van der Spek, H., and Nijtmans, L. G. (2003) The mitochondrial prohibitin complex is essential for embryonic viability and germline function in *Caenorhabditis elegans*. *J. Biol. Chem. 278*, 32091−32099.

(17) Mishra, S., Murphy, L. C., Nyomba, B. L., and Murphy, L. J. (2005) Prohibitin: A potential target for new therapeutics. *Trends Mol. Med. 11*, 192−197.

(18) Theiss, A. L., Obertone, T. S., Merlin, D., and Sitaraman, S. V. (2007) Interleukin-6 transcriptionally regulates prohibitin expression in intestinal epithelial cells. *J. Biol. Chem. 282*, 12804−12812.

(19) Bourges, I., Ramus, C., Moussonde Camaret, B., Beugnot, R., Remacle, C., Cardol, P., Hofhaus, G., and Issartel, J. P. (2004) Structural organization of mitochondrial human complex I: Role of the ND4 and ND5 mitochondria-encoded subunits and interaction with prohibitin. *Biochem. J. 383*, 491−499.

(20) Nijtmans, L.G., Artal, S. M., Grivell, L. A., and Coates, P. J. (2002) The mitochondrial PHB complex: Roles in mitochondrial respiratory complex assembly, ageing and degenerative disease. *Cell. Mol. Life Sci. 59*, 143−155.

(21) Dunn, K. C., Aotaki-Keen, A. E., Putkey, F. R., and Hjelmeland, L. M. (1996) ARPE-19, a human retinal pigment epithelial cell line with differentiated properties. *Exp. Eye Res. 62*, 155−169.

(22) Davis, A. A., Bernstein, P. S., Bok, D., Turner, J., Nachtigal, M., and Hunt, R. C. (1995) A human retinal pigment epithelial cell line that retains epithelial characteristics after prolonged culture. *Invest. Ophthalmol. Visual Sci. 36*, 955−964.

(23) Chung, H., Lee, H., Lamoke, F., Hrushesky, W. J., Wood, P. A., and Jahng, W. J. (2009) Neuroprotective role of erythropoietin by antiapoptosis in the retina. *J. Neurosci. Res. 87*, 2365−2374.

(24) Zhang, R., Hrushesky, W. J., Wood, P. A., Lee, S. H., Hunt, R. C., and Jahng, W. J. (2010) Melatonin reprogrammes proteomic profile in light-exposed retina in vivo. *Int. J. Biol. Macromol. 47*, 255−260.

(25) Lee, H., Chung, H., Arnouk, H., Lamoke, F., Hunt, R. C., Hrushesky, W. J., Wood, P. A., Lee, S. H., and Jahng, W. J. (2010) Cleavage of the retinal pigment epithelium-specific protein RPE65 under oxidative stress. *Int. J. Biol. Macromol. 47*, 104−108.

(26) Lee, H., Chung, H., Lee, S. H., and Jahng, W. J. (2011) Light-induced phosphorylation of crystallins in the retinal pigment epithelium. *Int. J. Biol. Macromol. 48*, 194−201.

(27) Cox, B., and Emili, A. (2006) Tissue subcellular fractionation and protein extraction for use in mass-spectrometry-based proteomics. *Nat. Protoc. 1*, 1872−1878.

(28) Osman, C., Haag, M., Potting, C., Rodenfels, J., Dip, P. V., Wieland, F. T., Brügger, B., Westermann, B., and Langer, T. (2009) The genetic interactome of prohibitins: Coordinated control of cardiolipin and phosphatidylethanolamine by conserved regulators in mitochondria. *J. Cell Biol. 184*, 583−596.

(29) van Gestel, R. A., Rijken, P. J., Surinova, S., O'Flaherty, M., Heck, A. J., Killian, J. A., de Kroon, A. I., and Slijper, M. (2010) The influence of the acyl chain composition of cardiolipin on the stability of mitochondrial complexes; an unexpected effect of cardiolipin in α-ketoglutarate dehydrogenase and prohibitin complexes. *J. Proteomics 73*, 806−814.

(30) Shigenaga, M. K., Hagen, T. M., and Ames, B. N. (1994) Oxidative damage and mitochondrial decay in aging. *Proc. Natl. Acad. Sci. U.S.A. 91*, 10771−10778.

(31) Ande, S. R., and Mishra, S. (2010) Palmitoylation of prohibitin at cysteine 69 facilitates its membrane translocation and interaction with Eps 15 homology domain protein 2 (EHD2). *Biochem. Cell Biol. 88*, 553−558.

(32) Morrow, I. C., Rea, S., Martin, S., Prior, I. A., Prohaska, R., Hancock, J. F., James, D. E., and Parton, R. G. (2002) Flotillin-1/reggie-2 traffics to surface raft domains via a novel golgi-independent pathway. Identification of a novel membrane targeting domain and a role for palmitoylation. *J. Biol. Chem. 277*, 48834−48841.

(33) Xue, L., Gollapalli, D. R., Maiti, P., Jahng, W. J., and Rando, R. R. (2004) A palmitoylation switch mechanism in the regulation of the visual cycle. *Cell 117*, 761−771.
(34) Artal-Sanz, M., and Tavernarakis, N. (2009) Prohibitin couples diapause signalling to mitochondrial metabolism during ageing in *C. elegans*. *Nature 461*, 793−797.
(35) Patel, N., Chatterjee, S. K., Vrbanac, V., Chung, I., Mu, C. J., Olsen, R. R., Waghorne, C., and Zetter, B. R. (2010) Rescue of paclitaxel sensitivity by repression of Prohibitin1 in drug-resistant cancer cells. *Proc. Natl. Acad. Sci. U.S.A. 107*, 2503−2508.
(36) Zubovych, I., Doundoulakis, T., Harran, P. G., and Roth, M. G. (2006) A missense mutation in *Caenorhabditis elegans* prohibitin 2 confers an atypical multidrug resistance. *Proc. Natl. Acad. Sci. U.S.A. 103*, 15523−15528.
(37) Terashima, M., Kim, K. M., Adachi, T., Nielsen, P. J., Reth, M., Köhler, G., and Lamers, M. C. (1994) The IgM antigen receptor of B lymphocytes is associated with prohibitin and a prohibitin-related protein. *EMBO J. 13*, 3782−3792.
(38) Nuell, M. J., Stewart, D. A., Walker, L., Friedman, V., Wood, C. M., Owens, G. A., Smith, J. R., Schneider, E. L., Dell'Orco, R., Lumpkin, C. K., Danner, D. B., and McClung, J. K. (1991) Prohibitin, an evolutionarily conserved intracellular protein that blocks DNA synthesis in normal fibroblasts and HeLa cells. *Mol. Cell. Biol. 11*, 1372−1381.
(39) Gregory-Bass, R. C., Olatinwo, M., Xu, W., Matthews, R., Stiles, J. K., Thomas, K., Liu, D., Tsang, B., and Thompson, W. E. (2008) Prohibitin silencing reverses stabilization of mitochondrial integrity and chemoresistance in ovarian cancer cells by increasing their sensitivity to apoptosis. *Int. J. Cancer 122*, 1923−1930.
(40) Ko, K. S., Tomasi, M. L., Iglesias-Ara, A., French, B. A., French, S. W., Ramani, K., Lozano, J. J., Oh, P., He, L., Stiles, B. L., Li, T. W., Yang, H., Martínez-Chantar, M. L., Mato, J. M., and Lu, S. C. (2010) Liver-specific deletion of prohibitin 1 results in spontaneous liver injury, fibrosis, and hepatocellular carcinoma in mice. *Hepatology 52*, 2096−2108.
(41) Ande, S. R., and Mishra, S. (2009) Prohibitin interacts with phosphatidylinositol 3,4,5-triphosphate (PIP3) and modulates insulin signaling. *Biochem. Biophys. Res. Commun. 390*, 1023−1028.
(42) Vessal, M., Mishra, S., Moulik, S., and Murphy, L. J. (2006) Prohibitin attenuates insulin-stimulated glucose and fatty acid oxidation in adipose tissue by inhibition of pyruvate carboxylase. *FEBS J. 273*, 568−576.
(43) Coates, P.J., Jamieson, D. J., Smart, K., Prescott, A. R., and Hall, P. A. (1997) The prohibitin family of mitochondrial proteins regulate replicative lifespan. *Curr. Biol. 7*, 607−610.
(44) Artal-Sanz, M., Tsang, W. Y., Willems, E. M., Grivell, L. A., Lemire, B. D., van der Spek, H., and Nijtmans, L. G. (2003) The mitochondrial prohibitin complex is essential for embryonic viability and germline function in *Caenorhabditis elegans*. *J. Biol. Chem. 278*, 32091−32099.
(45) Sánchez-Quiles, V., Santamaría, E., Segura, V., Sesma, L., Prieto, J., and Corrales, F. J. (2010) Prohibitin deficiency blocks proliferation and induces apoptosis in human hepatoma cells: Molecular mechanisms and functional implications. *Proteomics 10*, 1609−1620.
(46) Rajalingam, K., Wunder, C., Brinkmann, V., Churin, Y., Hekman, M., Sievers, C., Rapp, U. R., and Rudel, T. (2005) Prohibitin is required for Ras-induced Raf-MEK-ERK activation and epithelial cell migration. *Nat. Cell Biol. 7*, 837−843.
(47) Fusaro, G., Dasgupta, P., Rastogi, S., Joshi, B., and Chellappan, S. (2003) Prohibitin induces the transcriptional activity of p53 and is exported from the nucleus upon apoptotic signaling. *J. Biol. Chem. 278*, 47853−47861.
(48) Ikonen, E., Fiedler, K., Parton, R. G., and Simons, K. (1995) Prohibitin, an antiproliferative protein, is localized to mitochondria. *FEBS Lett. 358*, 273−277.
(49) Shi, S. L., Li, Q. F., Liu, Q. R., Xu, D. H., Tang, J., Liang, Y., Zhao, Z. L., and Yang, L. M. (2009) Nuclear matrix protein, prohibitin, was down-regulated and translocated from nucleus to cytoplasm during the differentiation of osteosarcoma MG-63 cells induced by ginsenoside Rg1, cinnamic acid, and tanshinone IIA (RCT). *J. Cell. Biochem. 108*, 926−934.
(50) Dong, P., Flores, J., Pelton, K., and Solomon, K. R. (2010) Prohibitin is a cholesterol-sensitive regulator of cell cycle transit. *J. Cell. Biochem. 111*, 1367−1374.
(51) Di, C., Xu, W., Su, Z., and Yuan, J. S. (2010) Comparative genome analysis of PHB gene family reveals deep evolutionary origins and diverse gene function. *BMC Bioinf. 11* (Suppl. 6), S22.